SUPPLEMENTARY MATERIAL

Additional Methods

Generation of Knockin Mouse Lines

Knockin mouse lines were generated by inserting a 2A-CreER or 2A-Flp cassette in-frame before the STOP codon of the targeted gene.

Targeting vectors were generated using PCR-based cloning approach as described before. Briefly, for each gene of interest, two partially overlapping BAC clones from the RPCI-23&24 library (made from C57BL/b mice) were chosen from the Mouse Genome Browser. 5' and 3' homology arms were PCR amplified (2-5kb upstream and downstream, respectively) using the BAC DNA as template and cloned into a building vector to flank the 2A-CreERT2 or 2A-Flp expressing cassette described in Taniguchi et al 2011. These targeting vectors were purified, tested for integrity by enzyme restriction and PCR sequencing. Linearized targeting vectors were electroporated into a 129SVj/B6 hybrid ES cell line (v6.5). ES clones were first screened by PCR and then confirmed by Southern blotting using appropriate probes. DIG-labeled Southern probes were generated by PCR, subcloned, and tested on wild-type genomic DNA verify that they give clear and expected results. Positive v6.5 ES cell clones were used for tetraploid complementation to obtain male heterozygous mice following standard procedures. The F0 males were bred with reporter lines (Supplementary Table S4) and induced with tamoxifen at the appropriate ages to characterize the resulting genetically targeted recombination patterns.

Tamoxifen Induction

Tamoxifen (T5648, Sigma) was prepared by dissolving in corn oil (20 $mg \bullet ml^{-1}$), applying a sonication pulse for 60 s, followed by constant rotation overnight at 37ºC. For embryonic induction, E0.5 was established as noon on the day of vaginal plug and tamoxifen was administered to pregnant mothers by gavage at a dose varying from 2-100 $mg \bullet kg^{-1}$ at the appropriate age. For postnatal induction, a 100-200 $mg \bullet kg^{-1}$ dose was administered by intraperitoneal injection at the appropriate age.

Immunohistochemistry

Embryonic brains were collected in PBS and fixed in 4% paraformaldehyde (PFA) 4h at room temperature, rinsed three times, dehydrated in 30% sucrose, frozen in OCT compound and cut by cryostat (Leica, CM3050S) in 20-50µm coronal sections. Postnatal mice aged 1-2 months were anesthetized using Avertin and intracardially perfused with saline followed by 4% PFA in PBS; brains were post-fixed in 4% PFA overnight at 4 °C and subsequently rinsed three times, embedded in 3% agarose-PBS and cut 50–100 µm in thickness using a vibrating microtome (Leica, VT100S). Sections were placed in blocking solution containing 10% Normal Goat Serum (NGS) and 0.1% Triton-X100 in PBS1X for 1 hr, then incubated overnight at 4 °C with primary antibodies diluted blocking solution. Sections were rinsed 3 times in PBS and incubated for 1 h at room temperature with corresponding secondary antibodies (1:500, Life Technologies). Sections were washed three times with PBS and incubated with DAPI for 5 min (1:5,000 in PBS, Life Technologies, 33342) to stain nuclei. Sections were dry-mounted on slides using Vectashield (Vector Labs, H1000) or Fluoromount (Sigma, F4680) mounting medium.

To perform molecular characterization of GeneX-CreER mouse lines, we stained 40µm vibratome sections for Cux1 and Ctip2, that were imaged in a Nikon Eclipse 90i fluorescence microscope.

Focusing on the somatosensory cortex, we counted tdTomato+ cells in a ~300µm width column and determined their relative position along the dorso-ventral axis that goes from the ventricular surface (0) to the pia (100%). As a reference, Ctip2+ and Cux1+ regions were plotted as green and blue bars, where the upper limits correspond to the mean relative position of the dorsal-most positive cells, and the lower limits correspond to the mean relative position of the ventral-most positive cells. Gray areas in histograms correspond to SD of those limits. The frequency of tdTomato+ cells along the dorso-ventral axis was plotted in a histogram with a bin width of 5%. Number of cells: Fezf2-CreER: 2781 cells, Tcerg1l-CreER: 185 cells, Adcyap1-CreER: 54 cells, Tle4-CreER: 2737 cells. For each line we quantified at least 4 sections from 2 embryos. Differences in cell numbers are due to differences in labeling density.
For colocalization determination, we obtained confocal z stacks centered in layer 5 or 6 of the somatosensory cortex, of 320x320x40µm^3 volumes. For all tdTomato+ cells in the volume we manually determined whether they were also positive for the desired markers by looking in individual z planes. The percentage of positive cells was calculated for each area. Number of tdTomato+ cells quantified per staining: Fezf2-CreER: ~200 cells per layer, Tcerg1lCreER: ~35 cells, Adcyap-CreER: ~10 cells, Tle4-CreER: ~100 cells in layer 5, ~550 in layer 6. For each line we quantified at least 4 sections from 1 embryo. Differences in cell numbers are due to differences in labeling density.

Antibodies
Anti-GFP (1:1000, Aves, GFP-1020); anti-RFP (1:1000, Rockland Pharmaceuticals, 600-401-379); anti-mKate2 for Brainbow 3.0 (gift of Dr. Dawen Cai, U Michigan); anti-Satb2 (1:20, Abcam ab51502); anti-CTIP2 (1:100, Abcam 18465); anti-CUX1 (1:100, SantaCruz 13024); anti-Ldb2 (1:200, Proteintech 118731-AP); anti-Fog2 (1:500, SantaCruz m-247) were used.

Virus
Adeno-associated viruses (AAVs) serotype 8, 9, DJ PHP.eB or retro2 packaged by commercial vector core facilities (UNC Vector Core, ETH Zurich, Biohippo, Penn, Addgene, …) were used as listed in Supplementary Table 2. Briefly, for cell-type specific anterograde tracing, we used either Cre- or Flp-dependent or tTA-activated AAVs combined with the appropriate reporter mouse lines (Supplementary Table 4)[1], or dual-tTA (Fig. 5 & 6) to express EGFP, EYFP or mRuby2 in labeled axons. Retrograde retroAAV2-Flp was used to infect axons at their terminals[6] in target brain structures to label PyNs retrogradely according to experiments detailed in Supplementary Table 2.

Viral Injection and Analysis
Stereotaxic viral injection
Adult mice were anesthetized by inhalation of 2% isofluorane delivered with a constant air flow (0.4 L•min^{-1}). Ketoprofen (5 mg•kg^{-1}) and dexamethasone (0.5 mg•kg^{-1}) were administered subcutaneously as preemptive analgesia and to prevent brain edema, respectively, prior to surgery, and lidocaine (2-4 mg•kg^{-1}) was applied intra-incisionally. Mice were mounted in a stereotaxic headframe (Kopf Instruments, 940 series or Leica Biosystems, Angle Two). Stereotactic coordinates were identified (Supplementary Table 2). An incision was made over the scalp, a small burr hole drilled in the skull and brain surface exposed. Injections were performed according to the strategies delineated in Supplementary Table 2. A pulled glass pipette tip of 20–30 µm containing the viral suspension was lowered into the brain; a 300-400 nl volume was delivered at

a rate of 30 nl•min^{-1} using a Picospritzer (General Valve Corp); the pipette remained in place for 10 min preventing backflow, prior to retraction, after which the incision was closed with 5/0 nylon suture thread (Ethilon Nylon Suture, Ethicon Inc. Germany) or Tissueglue (3M Vetbond), and animals were kept warm on a heating pad until complete recovery.

Systemic AAV injection
Foxp2-IRES-Cre mice were injected through the lateral tail vein at 4 weeks of age with 100 µl total volume of AAV9-CAG-DIO-EGFP (UNC Viral Core) diluted in PBS (5x1011 vg/mouse). Three weeks postinjection, mice were transcardially perfused with 0.9% saline, followed by ice-cold 4% PFA in PBS, and processed for STP tomography.

Microscopy
Imaging from serially mounted sections was performed on a Zeiss LSM 780 or 710 confocal microscope (CSHL St. Giles Advanced Microscopy Center) and Nikon Eclipse 90i fluorescence microscope, using objectives X63 and x5 for embryonic tissue, and x20 for adult tissue, as well as x5 on a Zeiss Axioimager M2 System equipped with MBF Neurolucida Software (MBF).

Whole-brain STP imaging
We used the whole-brain STP tomography pipeline previously described [4,5]. Perfused and post-fixed brains from adult mice, prepared as described above, were embedded in 4% oxidized-agarose in 0.05M PB, cross-linked in 0.2% sodium borohydrate solution (in 0.05 M sodium borate buffer, pH 9.0-9.5).The entire brain was imaged in coronal sections with a 20x Olympus XLUMPLFLN20XW lens (NA 1.0) on a TissueCyte 1000 (Tissuevision) with a Chameleon Ultrafast-2 Ti: Sapphire laser (Coherent). EGFP/EYFP or tdTomato signals were excited at 910 nm or 920 nm, respectively. Whole brain image sets were acquired as series of 12 (x) x 16 (y) tiles with 1 µm x 1 µm sampling for 230-270 z sections with a 50-µm z-step size. Images were collected by two PMTs (PMT, Hamamatsu, R3896), for signal and autofluorescent background, using a 560 nm dichroic mirror (Chroma, T560LPXR) and band pass filters (Semrock FF01-680/SP-25). The image tiles were corrected to remove illumination artifacts along the edges and stitched as a grid sequence [5,7]. Image processing was completed using ImageJ/FIJI and Adobe/Photoshop software with linear level and nonlinear curve adjustments applied only to entire images.

Cell body detection from whole-brain STP data
PyN somata were automatically detected from cell-type specific reporter lines (R26-LSL-GFP or Ai14) by a convolutional network trained as described in [8]. Detected PyN soma coordinates were overlaid on a mask for cortical depth, as described [8].

Axon detection from whole-brain STP data
For axon projection mapping, PyN axon signal based on cell-type specific viral expression of EGFP or EYFP was filtered by applying a square root transformation, histogram matching to the original image, and median and Gaussian filtering using Fiji/ImageJ software [9] so as to maximize signal detection while minimizing background auto-fluorescence, as described in [10]. A normalized substraction of the autofluorescent background channel was applied and the resulting thresholded images were converted to binary maps. 3D rendering was performed based on binarized axon projections and surfaces were determined based on the binary images using Imaris software

(Bitplane). Projections were quantified as the fraction of pixels in each brain structure relative to each whole projection.

Registration of whole-brain STP image datasets

Registration brain-wide datasets to the Allen reference Common Coordinate Framework (CCF) version 3 was performed by 3D affine registration followed by a 3D B-spline registration using Elastix software [11], according to parameters established by Ragan et al 2012 and Kim et al., 2015[4,5]. For cortical depth and axon projection analysis, we registered the CCFv3 to each dataset so as to report cells detected and pixels from axon segmentation in each brain structure without warping the imaging channel.

In vitro Electrophysiology

Brain slice preparation

Mice (>P30) were anesthetized with isoflurane, decapitated, brains dissected out and rapidly immersed in ice-cold, oxygenated, artificial cerebrospinal fluid (section ACSF: 110 mM choline-Cl, 2.5 mM KCl, 4mM MgSO4, 1mM CaCl2, 1.25 mM NaH2PO4, 26mM NaHCO3, 11mM D-glucose, 10 mM Na ascorbate, 3.1 Na pyruvate, pH 7.35, 300 mOsm) for 1 min. Coronal cortical slices containing somatomotor cortex were sectioned at 300 μm thickness using a vibratome (HM 650 V; Microm) at 1-2 °C and incubated with oxygenated ACSF (working ACSF; 124mM NaCl, 2.5 mM KCl, 2 mM MgSO4, 2 mM CaCl2, 1.25 mM NaH2PO4, 26 mM NaHCO3, 11 mM D-glucose, pH 7.35, 300mOsm) at 34 °C for 30 min, and subsequently transferred to ACSF at room temperature (25 °C) for >30 min before use. Whole cell patch recordings were directed to the somatosensory and motor cortex, the subcortical whiter matter and corpus callosum served as primary landmarks according to the atlas (Paxinos and Watson Mouse Brain in Stereotaxic Coordinates, 3rd edition).

Eletrophysiological recordings

Patch pipettes were pulled from borosilicate glass capillaries with filament (1.2 mm outer diameter and 0.69 inner diameter; Warner Instruments) with a resistance of 3-6 MΩ. The pipette recording solution consisted of 130 mM potassium gluconate, 15 mM KCl, 10 mM sodium phosphocreatine, 10 mM Hepes, 4 mM ATP·Mg, 0.3 mM GTP, and 0.3 mM EGTA (pH 7.3 adjusted with KOH, 300 mOsm). Dual or triple whole cell recordings from tdTomato+ and EGFP+ PyNs were made with Axopatch 700B amplifiers (Molecular Devices, Union City, CA) using an upright microscope (Olympus, Bx51) equipped with infrared-differential interference contrast optics (IR-DIC) and fluorescence excitation source. Both IR-DIC and fluorescence images were captured with a digital camera (Microfire, Optronics, CA). All recordings were performed at 33–34 °C with the chamber perfused with oxygenated working ACSF.

Recordings were made with two MultiClamp 700B amplifiers (Molecular Devices). The membrane potential was maintained at -75mV in the voltage clamping mode and zero holding current in the current clamping mode, without the correction of junction potential. Signals were recorded and filtered at 2 kHz, digitalized at 20 kHz (DIGIDATA 1322A, Molecular Devices) and further analyzed using the pClamp 10.3 software (Molecular Devices) for intrinsic properties.

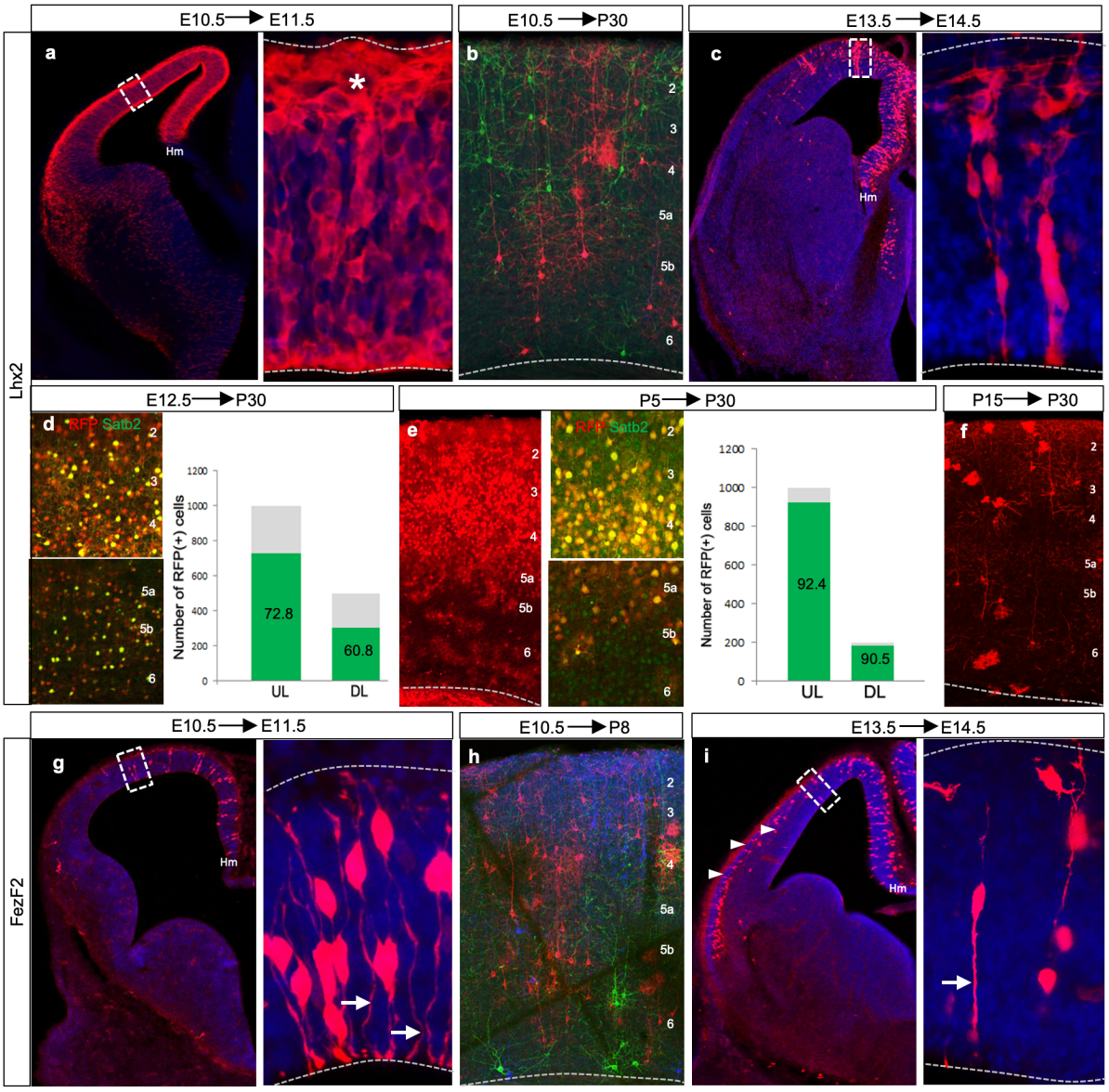

Extended Data Fig. 1: Fate mapping using two key developmental transcription factors. **a,** A full hemi-coronal view of E10.5 Lhx2$^+$ progenitors densely labeled throughout the dorsal neuroepithelium by 24-hour pulse-chase in a different *Lhx2-CreER;Ai14* mouse as in Fig.2e. Hm, cortex-hem boundary. High-magnification views show a dense post-mitotic layer (asterisk) below pia (dashed lines). **b,** Another example of fate mapping from E10.5 RGs to mature cortex using *Lhx2-CreER;RGBow* mice (as in Fig.2f). E10.5 Lhx2$^+$ RGs are multipotent and generate PyNs across layers. **c,** Another example of E13.5 Lhx2$^+$ RGs labeled by 24-hour pulse -chase using *Lhx2-CreER;Ai14* mice (Fig.2i). High-magnification view shows cell clones derived from individual RGs indicative of the rapid proliferation potential of Lhx2$^+$ RGs. **d,** Fate mapping E12.5 Lhx2$^+$RGs to mature cortex labeled PyN progeny that are SATB2$^+$ (IT class, 66.8%) as well as SATB2$^-$ (non-IT class, 33.2%). Quantification: 72.8% of L2-4 (UL; 728 of 1000 cells) and 60.8% of L5-6 (DL; 304 of 500 cells; n=3 brains from 2 litters) PyNs are of IT-type. **e**, P5 TM induction in *Lhx2-CreER;Ai14* shows dense labeling of L2-4 PyNs and sparse labeling in L5/6 in P28 cortex. Most labeled PyNs are of the IT class expressing SATB2 (UL, 92.4% - 924 of 1000 cells; DL,

90.5% - 181 of 200 cells; n=3 brains from 2 litters). **f,** P15 TM induction in *Lhx2-CreER;Ai14* mostly labeled astrocytes in mature cortex. **g,** At E10.5, *Fezf2*$^{+}$ RGs can only be sparsely labeled by 24-hour pulse-chase using another *FezF2-CreER;Ai14* mouse (as in Fig.2k). Magnified view shows RGs with endfeet (arrow) but sparsely labeled post-mitotic neurons (arrowheads), compared to those of Lhx2^{+} RGs at the same stage (SpplFig1a). **h,** Fate mapping E10.5 *Fezf2*$^{+}$RGs to P8 labeled PyNs across cortical layers in *Fezf2-CreER;RGBow* mice, indicating multi-potency of E10.5 *Fezf2*$^{+}$RGs. **i,** Another example of E13.5 *Fezf2*$^{+}$ RGs labeled by 24-hour pulse-chase in *Fezf2-CreER; Ai14* mice (Fig.2o). Magnified view shows sparsely labeled RGs, in sharp contrast to the highly prolific *Lhx2*$^{+}$ RGs at the same embryonic time (Sppl Fig1c).

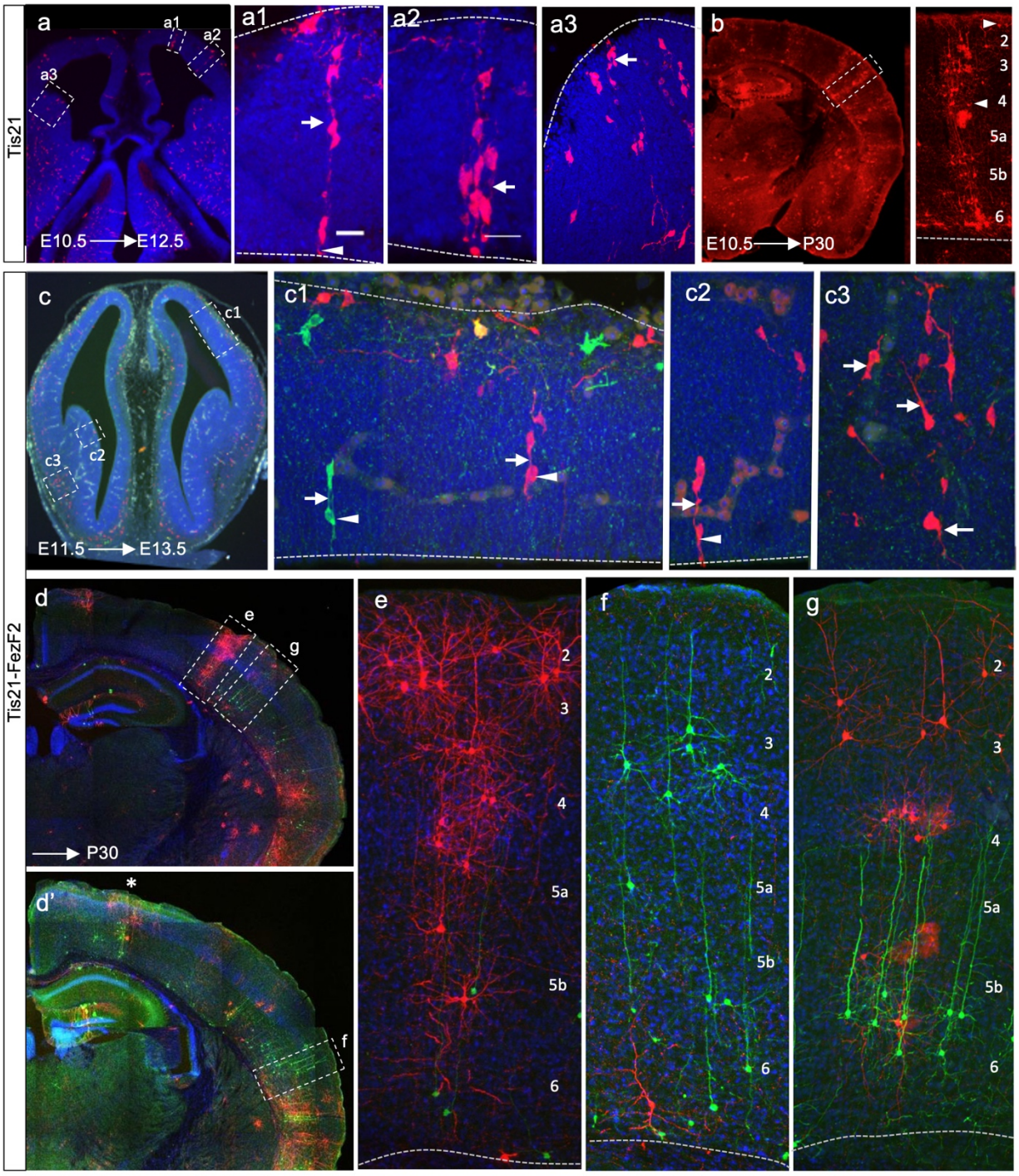

Extended Data Fig. 2: Strategy for simultaneous fate mapping using distinct molecularly defined progenitors. a, 48-hr pulse-chase in E10.5 *Tis21-CreER;Ai14* embryo labels *Tis21*$^{+}$ neurogenic progenitors and their postmitotic progeny throughout the neural tube, including dorsal pallium (a1) and ventral subpallium (a2). Self-renewing RGs identified by their endfeet at the ventricle surface (arrowheads) and radial fibers (arrow). **b,** Fate-mapping of E10.5 *Tis21*$^{+}$ nRGs to mature cortex reveals PyNs are distributed throughout cortical layers. Note that multipolar GABAergic interneurons (some in layer 1) derived from subpallium RGs are also labeled

(arrowheads). **c,** Differential labeling of *Tis21*$^+$ nRGs that are either *Fezf2*$^+$ or *Fezf2*$^-$ using an intersection/ subtraction strategy. 48-hr pulse-chase from *Tis21-CreER;Fezf2-Flp;IS2* embryo labeled *Tis21*$^+$*Fezf2*$^+$ RGs with GFP in dorsal pallium (c1), and *Tis21*$^+$*Fezf2*$^-$ RGs with RFP in both pallium (c2) and subpallium (c3). Migrating postmitotic neurons are indicated by arrows. **d,** Differential fate mapping of *Tis21*$^+$*Fezf2*$^+$ and *Tis21*$^+$*Fezf2*$^-$ RGs from E11.5 to the mature cortex using an intersection/subtraction strategy. The majority of clones consist of mixed RFP and GFP PyNs (asterisk, d'), and rarely RFP-only or GFP-only PyNs. **e,** RFP-only clones (1 of 29) likely derive from *Tis21*$^+$*Fezf2*$^-$ RGs whose progeny were all *Fezf2*$^-$. **f,** GFP-only clones (2 of 29) are derived from *Tis21*$^+$*Fezf2*$^+$ RGs, suggesting multipotency of *Fezf2*$^+$ RGs. **g,** Mixed RFP/GFP clones are most prominent and likely result from *Cre* activation of RFP in *Tis21*$^+$*Fezf2*$^-$ RGs and subsequent Flp activation of GFP in *Fezf2*$^+$ L5/6 postmitotic PyNs

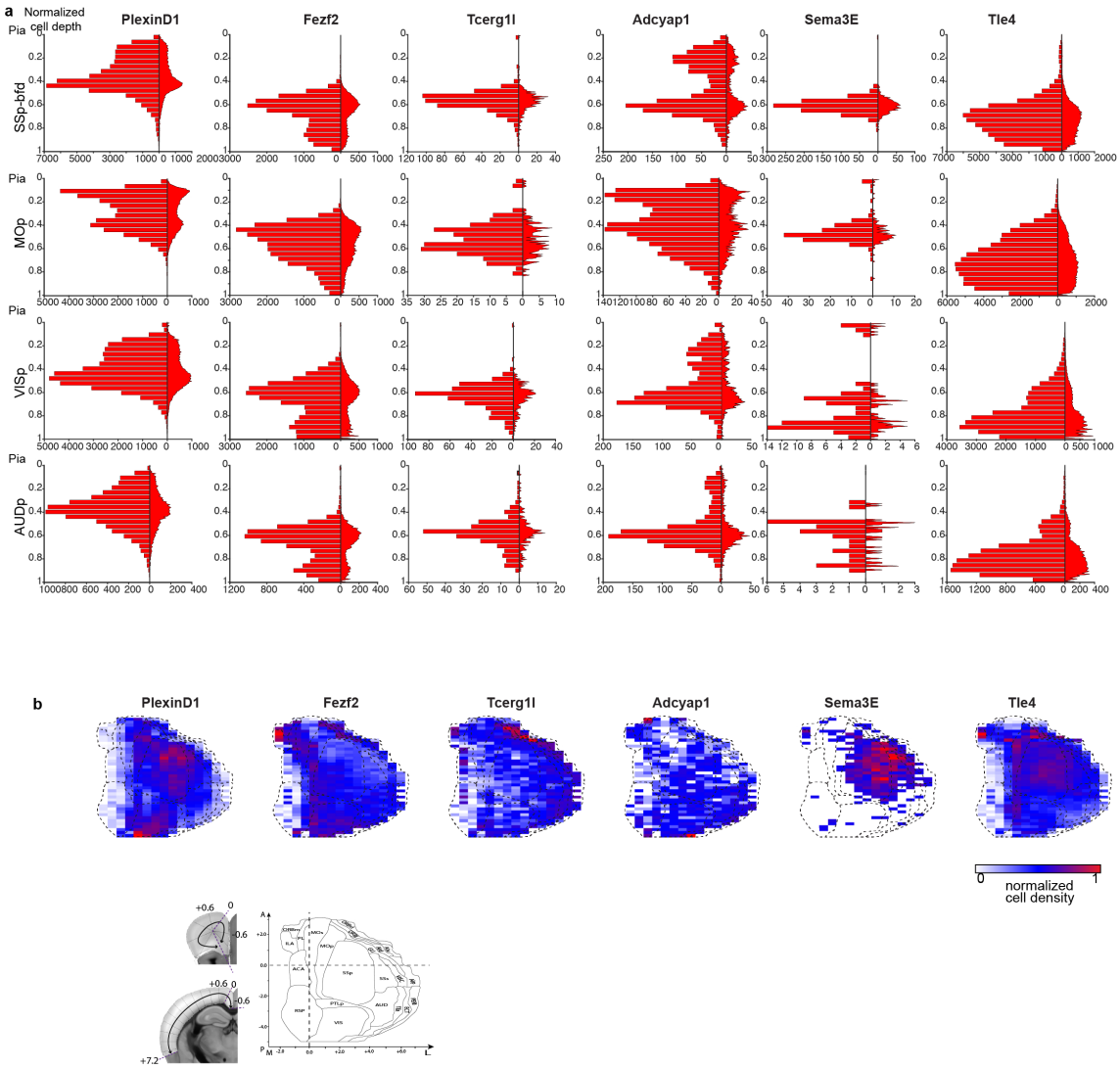

Extended Data Fig. 3 Cell distribution patterns of PyN subpopulations per cortical area. **a**, Histograms showing normalized laminar distribution for six genetically targeted PyN subpopulations by cortical area: primary somatoasensory (SSp), primary motor (Mop), primary visual (VISp) and primary auditory (AUDp). Brain-wide cortical depth quantification was performed based on cell detection by convolutional networks from *GeneX-CreER* driver lines crossed to *Ai14* (R26-LSL-tdTomato), *R26-LSL-h2b-GFP* or *Snap25-LSL-EGFP* reporters and induced at the ages specified in Fig. 3. The normalized cortical depth (0-1) was divided into 24 bins for the left histogram and 124 bins for the right plot. **b**, Interareal cortex-wide distribution pattern of PyN subpopulations normalized for each dataset's total number of cells detected, viewed as cortical flatmaps (upper row). Cortical flatmapping coordinate space (lower row).

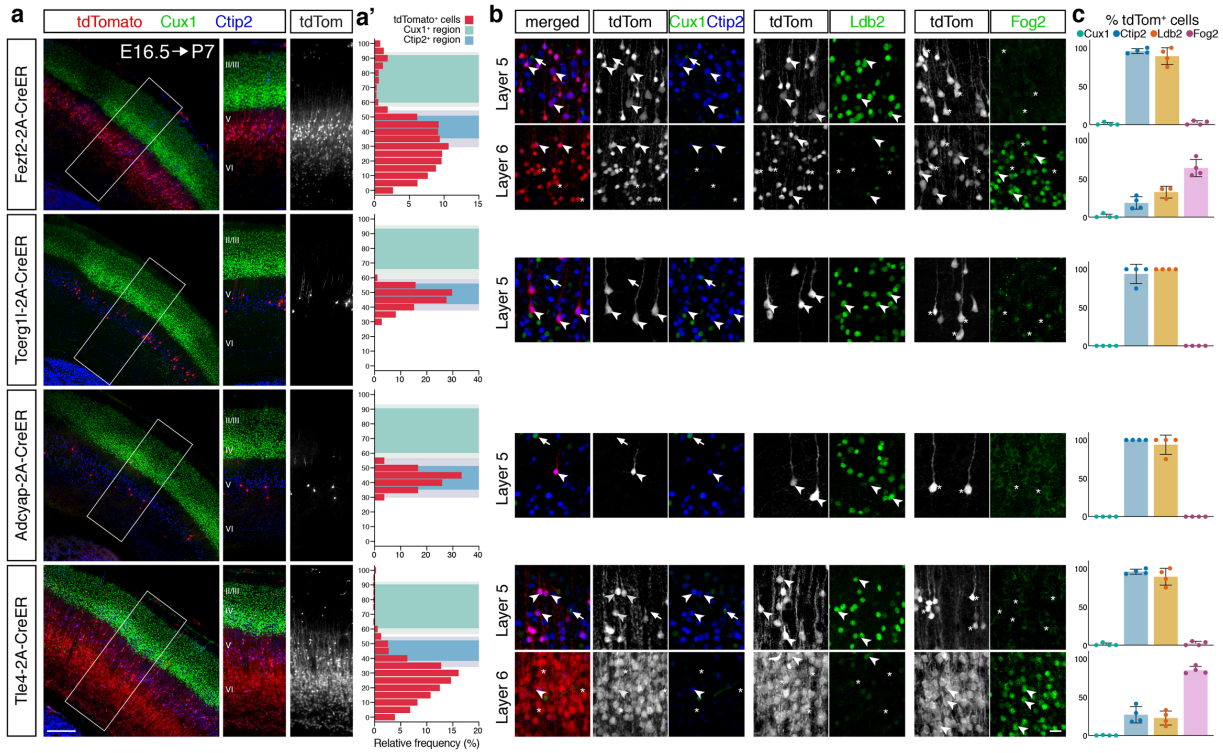

Extended Data Fig. 4 Molecular validation and characterization of 4 deep layer PyN driver lines. a, Low magnification images of coronal sections of somatosensory cortex at P7 stained with antibodies against Ctip2 and Cux1, and RFP fluorescence, from *GeneX-CreER* lines crossed to Ai14 reporter with TM induction at E16.5. Inset shows markers and RFP$^+$ cell distributions across layers. **a'**, Histograms of tdTomato$^+$ cell distribution in the cortical plate. Green and blue bars represent the areas occupied by Cux1$^+$ or Ctip2$^+$ cells, respectively. **b**, Magnification of RFP$^+$ cells in sections co-stained against Cux1 and Ctip2, Ldb2 (enriched in PT PyNs) and Fog2 (expressed in CT PyNs). Arrows designate double positive cells; asterisks denote tdTomato$^+$ cells not expressing the marker. **c**, Percentage RFP$^+$ cells stained with each antibody within somatosensory cortex in the specified layers. Each dot is an area, for which the percentage of double positive cells was calculated. Bars are mean+SD. Scalebars: a, 300µm; b, 20µm.

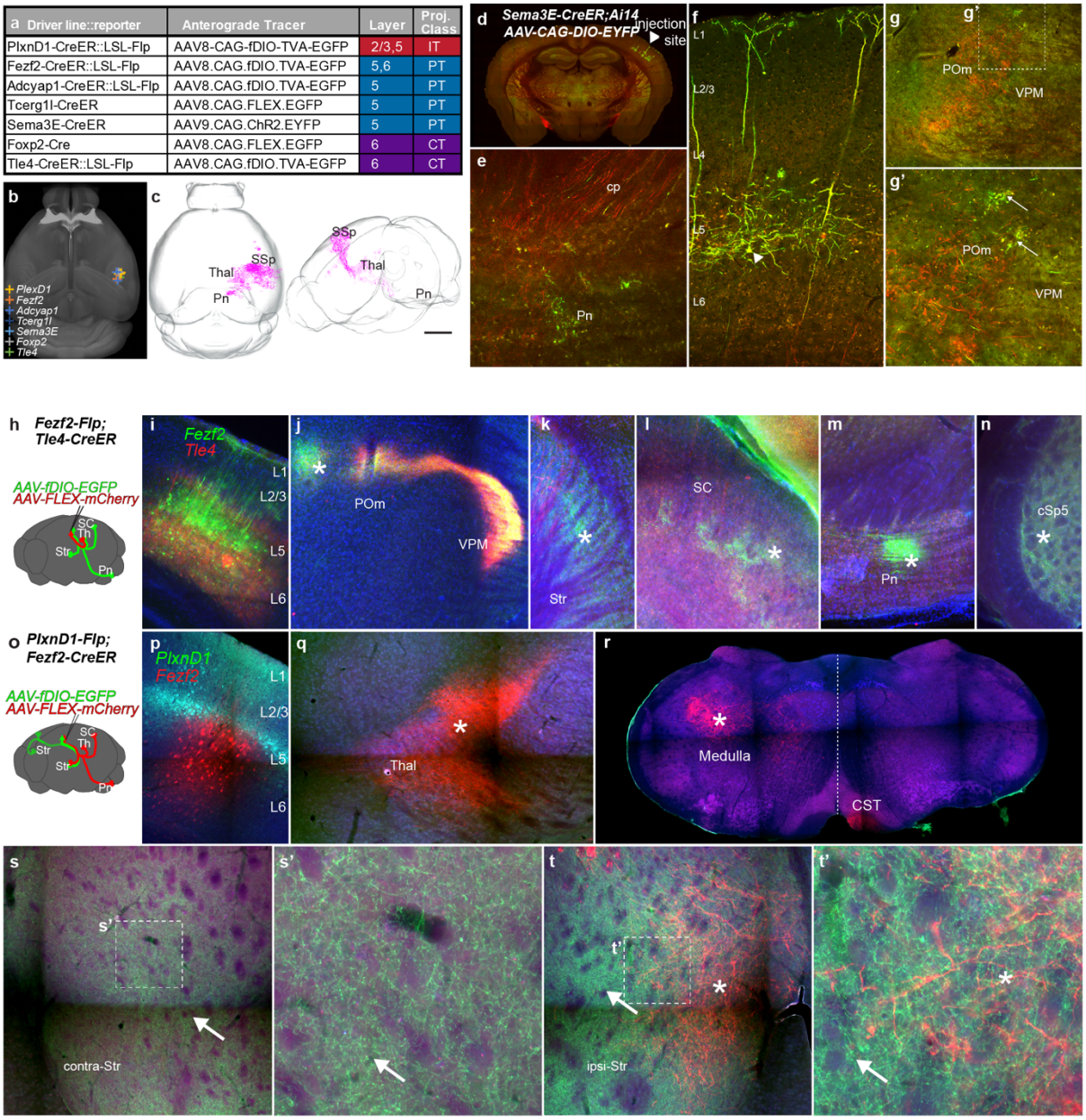

Extended Data Fig. 5. Anterograde tracing of axon projections from one or two PyN populations using single or double allele driver mice, respectively. a, Summary table of driver lines and viral vectors used for anterograde tracing from PyNs in primary somatosensory cortex, related to Fig. 4. **b**, Virus injection centroid coordinates across single driver experiments in CCFv3 space on a dorsal whole-brain view. **c**, 3D rendering of Sema3E projection pattern from STP imaging: dorsal view (left); parasagittal view (right). **d**, Coronal section containing injection site in a *Sema3E-CreER* brain. **e**, PyNs^{Sema3E} comprising a PT population project via the cerebral peduncle (cp) to pons (Pn). PyNs^{Sema3E} infected with AAV-DIO-GFP express EYFP; all other PyNs^{Sema3E} activated by TM induction express tdTomato. **f**, PyNs^{Sema3E} at injection site, showing somata in layer 5 with slender tufted apical dendrites. **g**, Axons in thalamus with large boutons in Pom (g'). **h-t**, Simultaneous anterograde tracing from two driver-defined PyN populations. **h**, Schematic showing simultaneous anterograted tracing from PyNs targeted by *Fezf2-Flp* (green)

and *Tle4-CreER* (red) with co-injection of Flp- and Cre- dependent AAVs expressing EGFP and mCherry, respectively (panels **i-n**). **i,** $PyNs^{Fezf2}$ and $PyNs^{Tle4}$ at the injection site occupying mainlyh L5B and L6, respectively. **j,** $PyNs^{Fezf2}$ and $PyNs^{Tle4}$ projection patterns converge in primary thalamus (VPM), while $PyNs^{Fezf2}$ collaterals extend medially to higher order thalamic nuclei. **k**, $PyNs^{Fezf2}$ (green) extend axon collaterals in striatum (Str), while $PyNs^{Tle4}$ (red) pass through en route to thalamus. **l-n**, $PyNs^{Fezf2}$ but not $PyNs^{Tle4}$ project to multiple other corticofugal targets, including superior colliculus (SC), pons (Pn) and contralateral spinal trigeminal nucleus (cSp5). **o**, Schematic showing simultaneous anterograde tracing from PyNs targeted by *PlxnD1-Flp* (green) and *Fezf2-CreER* (red) with co-injection of Flp- and Cre- dependent AAVs expressing EGFP and mCherry, respectively (panels **p-t**). **p**, $PyNs^{PlxnD1}$ and $PyNs^{Fezf2}$ at the injection site in motor cortex occupying mainly L5A and L5B/L6, respectively. **q-r**, $PyNs^{Fezf2}$ but not $PyNs^{PlxnD1}$ project to thalamus (Thal) (**q**) and medulla (**r**). **s-t,** $PyNs^{PlxnD1}$ and $PyNs^{Fezf2}$ project to ipsilateral striatum with overlapping terminals (**t**), while $PyNs^{PlxnD1}$ but not $PyNs^{Fezf2}$ project to contralateral striatum (**s**). PyN^{Fezf2} collaterals indicated with an asterisk (**j-t**); PyN^{PlxnD1} indicated with an arrow (**s-t**). Scale bars: **c**, 2 mm.

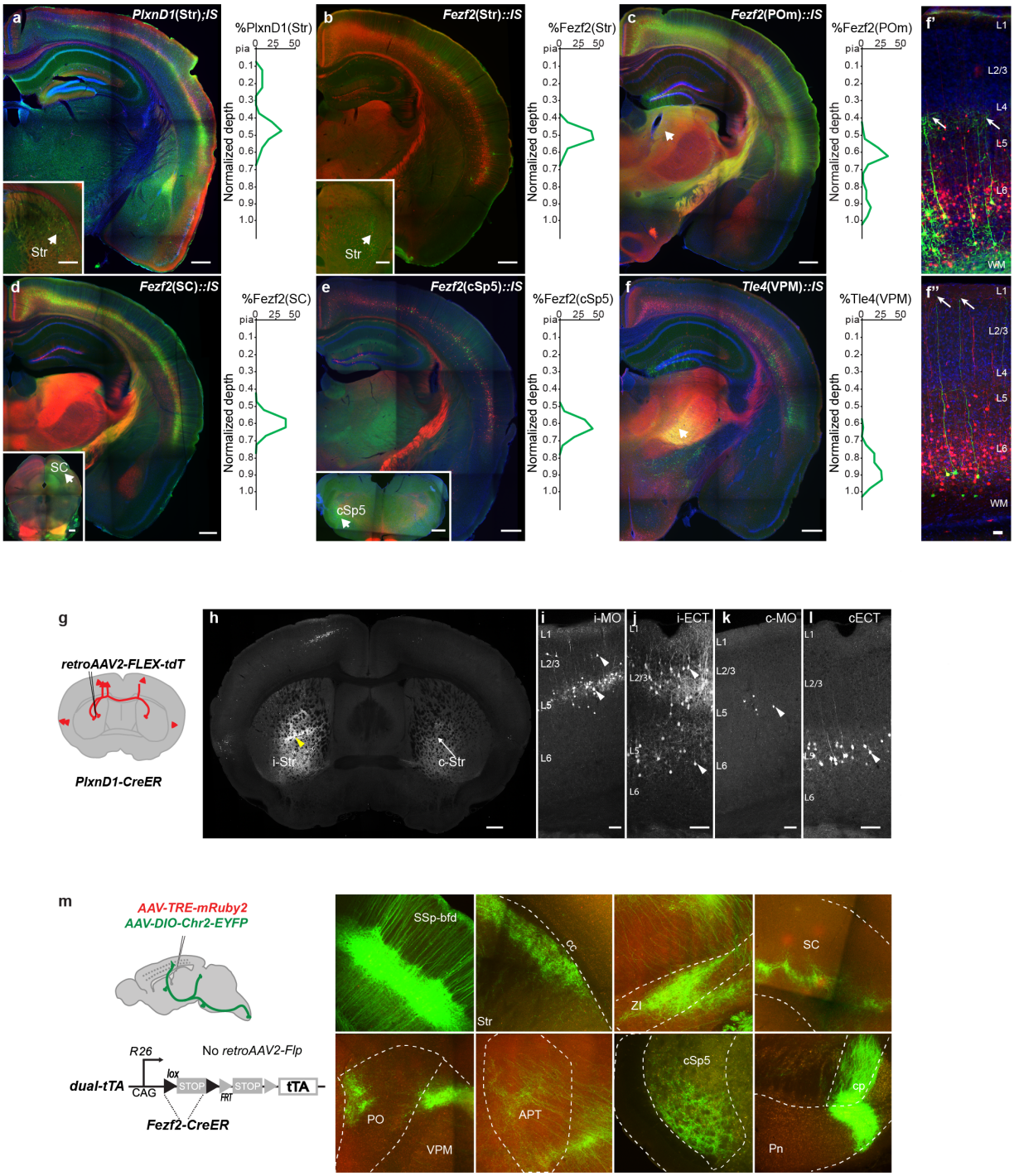

Extended Data Fig. 6. Retrograde and combinatorial targeting of PyN subpopulations.
a-f, Representative images illustrating injections of retroAAV2-retro-Flp (arrow heads) at subcortical targets of PlexD1, Fezf2 and Tle4 PyNs (insets in **a**, **b**, **d**, **e**), and retrograde labeling pattern from IS reporter recombination in hemisections containing somatosensory barrel field cortex (main image panel). Fezf2 hemisections correspond to image panels in Fig. 5c. Corresponding cortical soma depth distribution is shown to the right of each image panel (n=2 for each target). PyNs^{Tle4} projecting to the ventral posteromedial niucleus of thalamus (VPM) consist

of two subpopulations with apical dendrites in L4/5 (f') and L1 (f''), respectively, indicated by arrows. **g,** Retrograde targeting of striatum-projecting $PyNs^{PlxnD1}$ by injection of retroAAV2-FLEX-tdTomato in striatum. **h**, Coronal section displays injection site (arrowhead) and collaterals of retrogradely labeled $PyNs^{PlxnD1}$ in contralateral striatum (arrow). **i-l,** Laminar pattern of retrograde labled $PyNs^{PlxnD1}$ reveal what while L5A $PyNs^{PlxnD1}$ project to both ipsi- and contralateral side **(i, k, l)**), L2/3 $PyNs^{PlxnD1}$ mainly project to the ipsilateral striatum. **m,** Schematic of control experiment for use of Cre- and Flp-dependent dualtTA for target-defined axon projection mapping of $PyNs^{Fezf2}$ ('triple trigger'). Co-injection of a Cre-dependent AAV-DIO-ChR2-EYFP (green, positive control) and tTA-activated AAV-pHB-TRE-mRuby2 (red, negative control), followed by TM induction, in absence of Flp probes dependence of reporter on both Cre and Flp recombination. Example images of injectioj site (SSp-bfd) and axon projection targets of several indicated ipsi- and contra-lateral sites display $EGFP^{+}$ $PyNs^{Fezf2}$ axons from AAV dependent on Cre alone, but no $mRuby2^{+}$ axons, demonstrating the dependence of triple trigger strategy (**Fig. 5f**) on intersection of Cre and Flp. Scale bar in: a-h, 500µm; i-l, 100µm.

Category	Name	Targeting	Description
Driver	Lhx2-2A-CreER	*Lhx2* locus; 2A-CreER targeted before STOP codon	*LIM Homeobox 2*
	PlexinD1-2A-CreER	*PlexinD1* locus; 2A-CreER targeted before STOP codon	Plexin D1 receptor
	PlexinD1-2A-flpO	*PlexinD1* locus; 2A-FlpO targeted before STOP codon	
	Fezf2-2A-CreER	*Fezf2* locus; 2A-CreER targeted before STOP codon	*Fez family zinc finger 2 (Fezf2;* formerly known as *Fezl)*
	Fezf2-2A-flpO	*Fezf2* locus; 2A-FlpO targeted before STOP codon	
	Tcerg1l-2A-CreER	*Tcerg1l* locus; 2A-CreER targeted before STOP codon	*Transcription elongation regulator 1-like* (*Tcerg1l*)
	Adcyap1-2A-CreER	*Adcyap1* locus; 2A-CreER targeted before STOP codon	Adenylate cyclase activating polypeptide 1
	Sema3E-CreER	*Sema3E* locus; CreER fused to Sema3E at the ATG site (S. Arber)*	Sema domain, immunoglobulin domain (Ig), short basic domain, secreted, (semaphorin) 3E
	Tle4-2A-CreER	*Tle4* locus; 2A-CreER targeted before STOP codon	*Transducin-like enhancer of split 4* (*Tle4*), homolog of *Drosophila E(spl)*; also known as *Grg4*
	FoxP2-IRES-Cre	*FoxP2* locus; IRES-Cre targeted before STOP codon (R. Palmiter)	*Forkhead box P2*
	Tbr1-2A-CreER	*Tbr1* locus; 2A-CreER targeted before STOP codon	*T-Box, Brain 1*
	Cux1-2A-CreER	*Cux1* locus; 2A-CreER targeted before STOP codon	*Cut Like Homeobox 1*
	Tbr2-2A-CreER	*Tbr2* locus; 2A-CreER targeted before STOP codon	*T-box, Brain 2* (also known as *Eomes*)
	Tbr2-2A-FlpER	*Tbr2* locus; 2A-FlpER targeted before STOP codon	
	Tis21-ATG-CreER	*Tis21* locus; 2A-CreER targeted before STOP codon	*B-Cell Translocation Gene (BTG) Anti-Proliferation Factor; NGF-Inducible Anti-Proliferative Protein Pheochromacytoma Cell-3 (PC3)*
Reporter	dual-tTA	*Rosa* locus; Cag promoter; Intersection activator: Cre and Flp dependent; expresses tTA with ''Cre AND Flp'' intersection	

Table 1 Newly Generated Mouse Lines to target cortical PyNs.

Driver	OB	CX	HP	AMY	CNU	Septum	THAL	HT	Midbrain	Cb	BS	Retina
PlexinD1-2A-CreER. (TM P21/P28)		+++++	+	++	+++		-		-		+	++
PlexinD1-2A-flpO	++	+++++	+++	+++	+++	+?	-		-	++?	+	++
Fezf2-2A-CreER (TM P21/P28)	++	+++++	+++	++	+							++
Tcerg1l-2A-CreER. (TM P21/P28)	+	+++++				++		+++	+++ (&PAG)			++
Adcyap1-2A-CreER (TM PE17.5)	-	+++++	+	++	-		-	+	-	++	+++	++
Sema3E-CreER (TM E17.5, P7 or P21)		+++++									+	++
Tle4-2A-CreER (TM P21/P28)	++	+++++	+	+	+++	++	-	++	++	++	+	++
Tbr1-2A-CreER (TM P4)	+	++++	++++	+	++							?
Cux1-2A-CreER (TM P14/P21)	+++	++++	+-	+	+	++	++	+++	+++	+++	+	?
Foxp2 (Systemic AAV-CAG-DIO-EGFP at 2mo)	+	++++	-	+	++	+-	++++	+	++	++	+	?

Table 2 Overview of brain-wide expression patterns in cell bodies for each driver line. This table gives an overall impression of the recombination patterns in major adult brain regions in selected lines. Abbreviations: OB, olfactory bulb, HP, hippocampus, AMY, amygdala, CNU, cerebral nuclei, THAL, thalamus, HT, hypothalamus, Cb, cerebellum, BS, brainstem.

Supplementary tables

Supplementary tables with cell distribution and viral tracing experiment summaries, a full list of somatosensory axon targets and values measured from automated detection and other mouse lines used in the study will be available upon manuscript publication.

ADDITIONAL REFERENCES

1 He, M. *et al.* Strategies and Tools for Combinatorial Targeting of GABAergic Neurons in Mouse Cerebral Cortex. *Neuron* **91**, 1228-1243, doi:10.1016/j.neuron.2016.08.021 (2016).

2 Taniguchi, H. *et al.* A resource of Cre driver lines for genetic targeting of GABAergic neurons in cerebral cortex. *Neuron* **71**, 995-1013, doi:10.1016/j.neuron.2011.07.026 (2011).

3 Pecho-Vrieseling, E., Sigrist, M., Yoshida, Y., Jessell, T. M. & Arber, S. Specificity of sensory-motor connections encoded by Sema3e-Plxnd1 recognition. *Nature* **459**, 842-846, doi:10.1038/nature08000 (2009).

4 Kim, Y. *et al.* Mapping social behavior-induced brain activation at cellular resolution in the mouse. *Cell Rep* **10**, 292-305, doi:10.1016/j.celrep.2014.12.014 (2015).

5 Ragan, T. *et al.* Serial two-photon tomography for automated ex vivo mouse brain imaging. *Nat Methods* **9**, 255-258, doi:10.1038/nmeth.1854 (2012).

6 Tervo, D. G. *et al.* A Designer AAV Variant Permits Efficient Retrograde Access to Projection Neurons. *Neuron* **92**, 372-382, doi:10.1016/j.neuron.2016.09.021 (2016).

7 Preibisch, S., Saalfeld, S. & Tomancak, P. Globally optimal stitching of tiled 3D microscopic image acquisitions. *Bioinformatics* **25**, 1463-1465, doi:10.1093/bioinformatics/btp184 (2009).

8 Kim, Y. *et al.* Brain-wide Maps Reveal Stereotyped Cell-Type-Based Cortical Architecture and Subcortical Sexual Dimorphism. *Cell* **171**, 456-469 e422, doi:10.1016/j.cell.2017.09.020 (2017).

9 Schindelin, J. *et al.* Fiji: an open-source platform for biological-image analysis. *Nat Methods* **9**, 676-682, doi:10.1038/nmeth.2019 (2012).

10 Mandelbaum, G. *et al.* Distinct Cortical-Thalamic-Striatal Circuits through the Parafascicular Nucleus. *Neuron* **102**, 636-652 e637, doi:10.1016/j.neuron.2019.02.035 (2019).

11 Klein, S., Staring, M., Murphy, K., Viergever, M. A. & Pluim, J. P. elastix: a toolbox for intensity-based medical image registration. *IEEE Trans Med Imaging* **29**, 196-205, doi:10.1109/TMI.2009.2035616 (2010).